Pergamon

Int. J. Heat Mass Transfer. Vol. 40, No. 2, pp. 393–405, 1997

0017–9310/97 $15.00+0.00

PII: S0017-9310(96)00111-1

The effective thermal conductivity of a porous medium with interconnected particles

G. BUONANNO and A. CAROTENUTO

Dipartimento di Ingegneria Industriale, University of Cassino, 03043, Cassino, Italy

(*Received* 3 *August* 1995 *and in final form* 20 *February* 1996)

Abstract—The procedure of volume averaging is applied to the process of steady-state heat conduction in a two-phase system and a method is developed to calculate the effective thermal conductivity. This method provides details of solid mechanics and thermal problems, and particle–particle contact is treated in an empirical manner. The proposed method is applied for periodic regular arrangements of circular and square cylinders. The effects of particle shape, roughness and solid conductivity are examined. A qualitative comparison between theory and experiment is also reported. Copyright © 1996 Elsevier Science Ltd.

1. INTRODUCTION

The problem of determining the effective thermal conductivity of a composite medium or a multiphase system is of interest to a wide range of engineering problems. For instance, knowledge of it is essential to determine the temperature field in a packed bed reactor, in a non-isothermal catalyst pellet, in the thermal process of oil recovery and shale oil retorting operations and in the drying process. The existing theoretical treatment of effective conductivity is based on the local volume averaging method. In the following, we briefly review the approach used by Whitaker [1, 2] applied to the two-phase system illustrated in Fig. 1. The heat conduction problem is developed from the steady-state energy equation for the "s" and the "f" phases:

$$\nabla \cdot k_s \nabla T_s = 0 \quad \text{and} \quad \nabla \cdot k_f \nabla T_f = 0 \qquad (1)$$

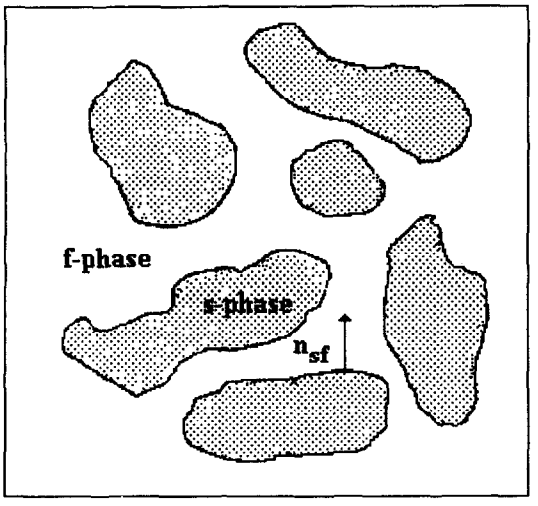

Fig. 1. Two-phase system.

with the boundary conditions on the s–f interfacial area A_{fs}:

$$\mathbf{n}_{fs} \cdot k_f \nabla T_f = \mathbf{n}_{fs} \cdot k_s \nabla T_s \quad \text{and} \quad T_f = T_s \qquad (2)$$

where k_s and k_f are the conductivity of the "s" and the "f" phases, respectively, $\mathbf{n}_{fs}$ is the unit normal vector outward from the fluid phase. By using the theory of local volume averaging assuming local thermal equilibrium [1, 3], and applying the averaging [4] and the modified averaging theorems [5], a single heat conduction equation is written as:

$$\nabla \left\{ [\phi k_f + (1-\phi) k_s] \nabla \langle T \rangle + \frac{k_f - k_s}{V} \int_{A_{fs}} \mathbf{n}_{fs} \tilde{T}_f \, dA \right\} = 0 \qquad (3)$$

where ϕ is the porosity of the porous medium, V is the averaging volume [6], $\langle T \rangle$ is the local volume averaged temperature defined as:

$$\langle T \rangle = \frac{1}{V} \int_V T \, dV = \phi \langle T_f \rangle^f + (1-\phi) \langle T_s \rangle^s \qquad (4)$$

where $\langle T_s \rangle^s$ and $\langle T_f \rangle^f$ are the intrinsic phase average temperatures of the "s" and "f" phases, respectively, and $\tilde{T}_f$ is the local deviation temperature of the "f" phase defined by Gray as [5]:

$$\tilde{T}_f = T_f - \langle T_f \rangle^f. \qquad (5)$$

Analogously the local deviation temperature $\tilde{T}_s$ of the "s" phase is defined as:

$$\tilde{T}_s = T_s - \langle T_s \rangle^s. \qquad (6)$$

A theoretical procedure to determine the local deviations $\tilde{T}_f$ and $\tilde{T}_s$ is developed in [7] in the form:

$$\tilde{T}_f = \mathbf{b}_f \cdot \nabla \langle T \rangle \quad \text{and} \quad \tilde{T}_s = \mathbf{b}_s \cdot \nabla \langle T \rangle \qquad (7)$$

where $\mathbf{b}_f$ and $\mathbf{b}_s$ are the two transformation vectors that

NOMENCLATURE

a	side length of square [m]
A	external surface of the cylinder [m^2]
A_{fs}	solid–fluid interfacial area [m^2]
$\mathbf{b}$	transformation vector [m]
c	width of contact area [m]
d	distance [m]
$\mathbf{f}$	elasticity material constant
E	Young's modulus [Pa]
G	average weight force per unit length [N]
h	thermal conductance for unit contact area [W m^{-2} K^{-1}]
H	height of packed bed [m]
$\mathbf{I}$	identity tensor
k	conductivity [W m^{-1} K^{-1}]
$\mathbf{K}_e$	effective conductivity tensor [W m^{-1} K^{-1}]
k_e	effective conductivity [W m^{-1} K^{-1}]
L	side length of unit cell [m]
L_c	length of cylinders [m]
$\mathbf{L}_i$	periodicity vector [m]
l	dimension of the slab [m]
$\mathbf{m}$	position vector [m]
N	number of row of cylinders
$\mathbf{n}_{fs}$	unit normal vector outward from fluid phase
P	pressure on nominal contact area [Pa]
$\mathbf{q}$	heat flux [W m^{-2}]
r	radius of circular cylinder [m]
R	thermal resistance [W K^{-1}]
S	boundary surface of packed bed [m^2]
$\mathbf{t}$	specific boundary stress [Pa]
T	temperature [K]
$\mathbf{u}$	displacement [m]
x, y	Cartesian coordinates [m]
X	x-direction
Y	y-direction
V	local representative elementary volume [m^3].

Greek symbols

δ	hardness [N m^{-2}]
ΔT	imposed difference temperature [K]
ε	strain component
ϕ	porosity
γ	strain component
σ	stress component [Pa]
θ_m	average angle of inclination
τ	stress component [Pa]
Π	contact area [m^2]
ν	Poisson ratio
Ψ	plasticity index
ξ	rugosity [m].

Subscripts

A	area
d	inferior surface of the packed bed
f	fluid
l	left surface of the packed bed
r	right surface of the packed bed
u	superior surface of the packed bed
s	solid
1	contact area on Y direction
2	contact area on X direction.

Superscripts

f	fluid
s	solid
~	deviation.

Other symbols

$\langle\rangle^f$	volume averaged over the fluid phase
$\langle\rangle^s$	volume averaged over the solid phase
$\langle\rangle$	volume averaged.

map $\nabla\langle T\rangle$ to $\tilde{T}_f$ and $\tilde{T}_s$, respectively. Consequently, substituting (7) in (3) the effective conductivity tensor is obtained by the equation:

$$\mathbf{K}_e = [\phi k_f + (1-\phi)k_s]\mathbf{I} + \frac{k_f - k_s}{V}\int_{A_{fs}} \mathbf{n}_{fs}\mathbf{b}_f \, dA. \quad (8)$$

In this case a single heat conduction equation can be written for the porous medium as:

$$\nabla\cdot(\mathbf{K}_e\cdot\nabla\langle T\rangle) = 0. \quad (9)$$

Vectors $\mathbf{b}_f$ and $\mathbf{b}_s$ are found by solving equations [7]:

$$\nabla^2\mathbf{b}_f = 0 \quad \text{and} \quad \nabla^2\mathbf{b}_s = 0. \quad (10)$$

with the boundary conditions on A_{fs}:

$$k_f\mathbf{n}_{fs}\cdot\nabla\mathbf{b}_f = k_s\mathbf{n}_{fs}\cdot\nabla\mathbf{b}_s + \mathbf{n}_{fs}(k_s - k_f). \quad (11)$$

It should be clear that the problem of (10) and (11) is nearly as complex as the original problem stated by (1) and (2).

Ryan *et al.* [8] have demonstrated that if the porous medium can be considered as being spatially periodic, so too are $\mathbf{b}_f$ and $\mathbf{b}_s$; in this hypothesis the solution to this problem can be obtained only in a representative unit cell of the porous medium. Under these circumstances the periodic boundary conditions are given by:

$$\mathbf{b}_f(\mathbf{m} + \mathbf{L}_i) = \mathbf{b}_f(\mathbf{m}) \quad (12)$$

where $\mathbf{m}$ is the position vector and $\mathbf{L}_i$ is the periodic vector.

The numerical solution to the problem for a periodic structure of in-line non-connected square cyl-

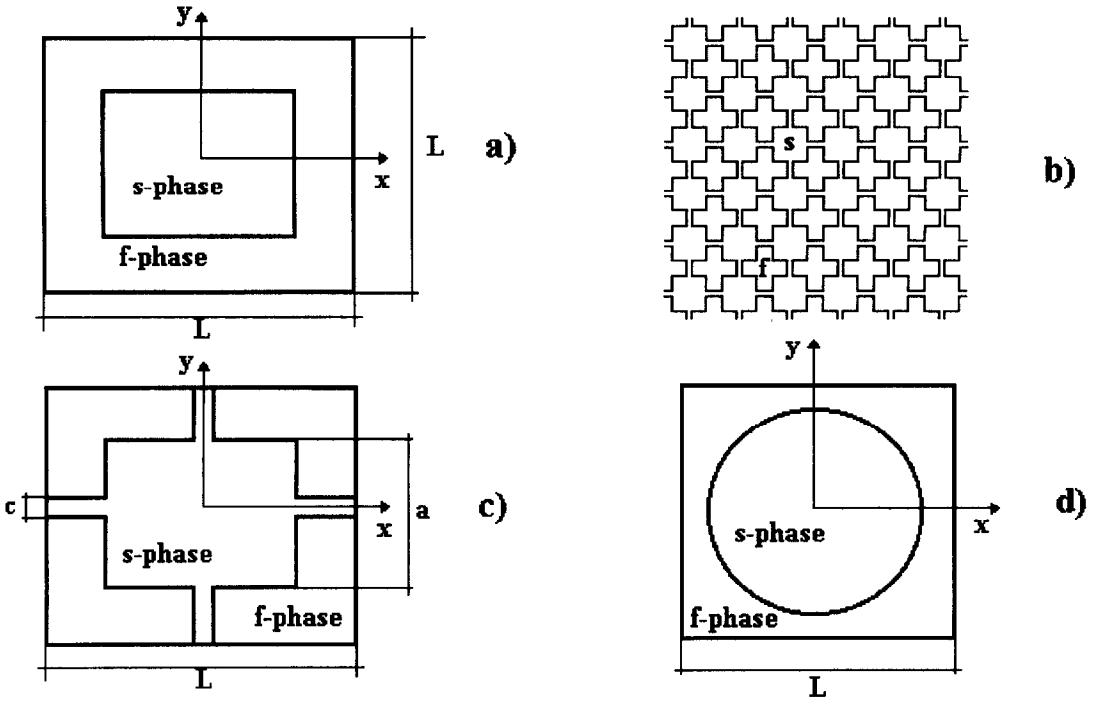

Fig. 2. (a) Unit cell for non-connected square cylinders, (b) regular packed bed of square cylinders, (c) unit cell for interconnected square cylinders, (d) unit cell for non-connected circular cylinders.

inders is obtained by Nozad *et al.* [7] on the unit cell as shown in Fig. 2(a) using the finite difference method. In particular, they found that the numerical solution is straightforward for moderate values of the ratio $k_s : k_f$, but for large values of this ratio the problem encounters numerical instabilities. These difficulties can be overcome using an *outer expansion* in the perturbation parameter $(k_s/k_f)^{-1}$. The results show that the effective thermal conductivity for non-touching cylinders is dominated by $k_s : k_f$ and ϕ and only slightly influenced by geometrical configuration.

To simulate the effect of particle–particle contact Nozad *et al.* [7] used the model of a spatially periodic porous medium illustrated in Fig. 2(b) with the unit cell shown in Fig. 2(c). In this case, the "s" phase is continuous and the contact effect is simulated using a slab of uniform thickness c, placed in the centre of each side.

The value of the ratio $c : a$ equal to 0.02, [where a is side length of square in Fig. 2(c)], was first suggested in [7]; it was used to compare the numerical results of effective conductivity with experimental values to simulate a porous medium with a porosity of $\phi = 0.36$. As noted in [9, 10], the inner expansion method proposed by Nozad *et al.* produced an overestimation of the contact area for values of $k_s/k_f > 10^4$ and consequently the value $c : a = 0.01$ was suggested [9, 10].

The experimental values used to determine $c : a$ are obtained from the results of different researchers for different beds (spheres and cylinders) with different arrangements (random and regular) using different solid particles (aluminium, bronze, stainless steel, glass, etc.) and stagnant fluids (air, water, helium, etc.).

To evaluate the effective thermal conductivity, Sahraoui and Kaviany proposed a different approach where $\mathbf{K}_e$ is computed directly from the temperature field [9]. The two-dimensional (2D) heat conduction is solved by using the finite-different method for the unit cells shown in Fig. 2(d) (non-connected particles) and Fig. 2(c) (interconnected particles), with periodic boundary conditions. The effective thermal conductivity is obtained by [9]:

$$\frac{k_e}{k_f} = \frac{\langle q_y \rangle_{A_x}\left(y = \frac{L}{2}\right)}{\Delta T} \tag{13}$$

where $\langle q_y \rangle_{A_x}$ is the area-averaged y-direction heat flux vector and ΔT is the temperature difference imposed as boundary condition.

In [9] the effects of $k_s : k_f$, porosity, and particle geometry and arrangement on the effective conductivity is examined in detail for non-connected particles using the unit cells shown in Figs. 2(a) and (d). Vice versa the case of interconnected particles is examined using only the unit cell of Fig. 2(c). The Saharaoui and Kaviany results show that the value $c : a = 0.01$ overpredicts the effective conductivity for a packed bed of spheres and the value of $c : a = 0.002$ is suggested for high values of $k_s : k_f$. This value is obtained using the experimental results presented in Nozad *et al.* [7] and in Jaguaribe and Beasley [11].

In conclusion, the effective thermal conductivity is predicted using a single value of $c : a$ as representing a

universal parameter for porous medium. This value is determined since it supplies the best reasonably good agreement between the theoretical results and all the experimental results of the different types of porous medium.

The above-described method, however, presents some unsolved problems, such as:

(i) high dispersion of the experimental results;
(ii) large differences of $\mathbf{K}_e$ values obtained in apparent identical experimental conditions (see Figs. 7–9); and
(iii) large differences between some experimental results and the corresponding numerical values (for instance, the aluminium–air system referred to in [7] and [10]).

These problems could be resolved using a procedure to determine different values of c according to the type of solid and fluid forming the porous medium. For this reason the authors propose a solution method to evaluate the effective thermal conductivity for a porous medium with interconnected particles which includes details of the solid mechanics problem.

2. SOLUTION METHOD

In general, the point-type or linear contacts between two bodies are purely theoretical; they presume that the solids in contact are perfectly rigid. In reality, when two non-conforming solid are brought in to contact they touch initially at a single point or along a line. Under the action of the slightest load they deform in the vicinity of their point of first contact so that they touch over an area which is finite though small compared with the dimensions of the two bodies.

Imposing the same temperature gradient as boundary condition the contact area dimension highly influences the thermal behaviour of the porous medium; when this dimension increases, the conduction heat flux across the solid particles, and, consequently, the effective thermal conductivity both increase if $k_s > k_f$ and, decrease if $k_s < k_f$.

Hence a theory of contact is necessary to predict the number, the position, the shape and the dimension of the contact areas and to determine the effective thermal conductivity. In general, the problem presents itself as being extremely complex since it is known that $\mathbf{K}_e$ is also a function of the shape of the solid matrix, of the porosity, of the type of arrangement of the particles and of the $k_s : k_f$ ratio.

We chose in this initial test of the theory to restrict ourselves to a simple possible computational problem; in particular, the determination of $\mathbf{K}_e$ is computed for a regular packed bed of circular or square cylinders which have a constant conductivity k_s and they are embedded in a stagnant fluid having a constant conductivity k_f. Moreover, we assume that the solid has a linear elastic behaviour; consequently, the solid mechanics problem is solved using the elastic theory of contact.

In this theory the contact surfaces are smooth and continuous hence the stresses are finite everywhere. The contact area determined using the elastic contact theory is defined as the nominal contact area [13].

In general, the contact between solid surfaces is discontinuous and the real area of contact is a small fraction of the nominal contact area. Moreover the topographical characteristics of the rough surfaces (profile, shape and height of the asperities) and their mechanical behaviour are relevant to determine the real macroscopic contact area. In particular the asperities can present elastic or plastic deformations depending on their microscopic geometry and on the mechanical properties of the solid. The proposed method determines as in a first step the nominal contact area using the elastic contact theory and then takes account of the real contact area in the thermal problem.

Despite the particular type of porous medium investigated, the results obtained can in any case furnish useful indications for later studies in the light of some of the considerations that have emerged in literature. In particular:

(1) in the analysis of properties of heterogeneous medium with random structure, it is customary to assume that the granular medium is statistically homogeneous [12]; and
(2) Saez *et al.* [14] in their study for a three-dimensional medium made of cubic particles report that for isotropic structures the effective conductivity depends only on the porosity and the 3D effects are not very important.

2.1. *Solid mechanics problem*

The solid mechanics problem consists in determining the final configuration of the contact area dimensions for each cylinder in the packed bed bounded, laterally and from below, by the plane walls of a container.

Since each cylinder is subject to different weight forces transmitted from laid-upon cylinders through the contact area, it is necessary to find the stress and the elastic displacement of any point of each cylinder. It is important to note that if the length of the cylinders is very large compared to the radius, then the solid mechanics problem can be simplified to a plane strain problem. In this hypothesis the equations governing the elastostatic problem are [13]:

equilibrium field equations:

$$\frac{\partial \sigma_x}{\partial x} + \frac{\partial \tau_{xy}}{\partial y} = 0 \tag{14}$$

$$\frac{\partial \sigma_y}{\partial y} + \frac{\partial \tau_{xy}}{\partial x} = 0 \tag{15}$$

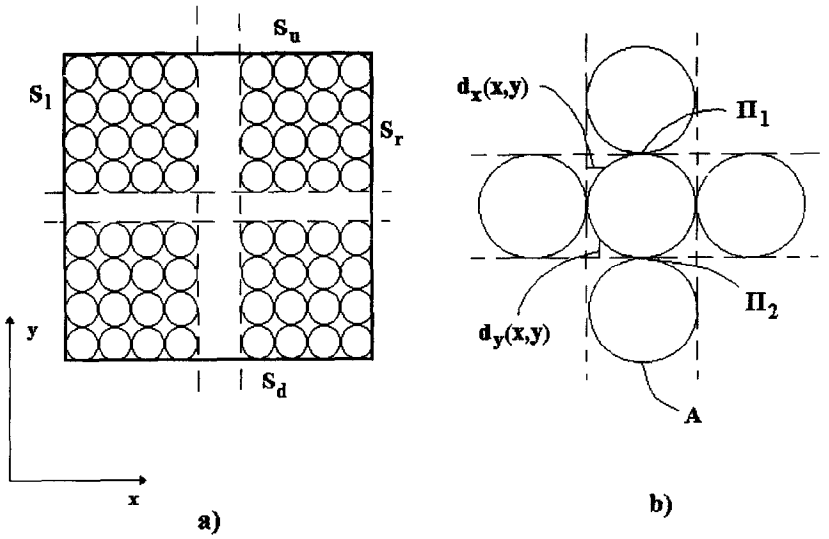

Fig. 3. (a) Regular packed bed of circular cylinders, (b) particular of regular packed bed of circular cylinders with the areas of contact indicated, (c) particular of regular packed bed of square cylinders with the dimensions c_1 and c_2 of the contact areas Π_1 and Π_2 indicated respectively and the distances d_x and d_y.

compatibility relationships:

$$\varepsilon_x = \frac{\partial u_x}{\partial x} \quad \varepsilon_y = \frac{\partial u_y}{\partial y} \quad \gamma_{xy} = \frac{\partial u_y}{\partial x} + \frac{\partial u_x}{\partial y} \tag{16}$$

constitutive relationships:

$$\begin{Bmatrix} \sigma_x \\ \sigma_y \\ \tau_{xy} \end{Bmatrix} = \begin{bmatrix} f_{11} & f_{12} & 0 \\ f_{12} & f_{22} & 0 \\ 0 & 0 & f_{66} \end{bmatrix} \begin{Bmatrix} \varepsilon_x \\ \varepsilon_y \\ 2\gamma_{xy} \end{Bmatrix} \tag{17}$$

where f_{ij} ($f_{ji} = f_{ij}$) are the elasticity (material) constants, σ_x, σ_y and τ_{xy} are the stress components, ε_x, ε_y and γ_{xy} are the strain components and u_x and u_y are the displacement components. For an isotropic material, f_{ij} can be expressed only in terms of the Young modulus E and the Poisson ratio ν as:

$$f_{11} = \frac{E(1-\nu)}{1-\nu-2\nu^2} \quad f_{22} = \frac{E(1-\nu^2)}{(1-\nu)(1-\nu-2\nu^2)}$$

$$f_{12} = \frac{\nu E}{1-\nu-2\nu^2} \quad f_{66} = \frac{E}{2(1+\nu)}. \tag{18}$$

Consider an assembly of a regular disposition of N-rows of cylinders represented in Fig. 3(a), the boundary conditions on the packed bed [Fig. 3(b)] are:

natural

$$t_y(x,y) = \tau_{xy}n_y + \sigma_y n_y < 0 \quad \text{on } \Pi_1(x,y) \tag{19}$$

$$t_x(x,y) = \tau_{xy}n_x + \sigma_x n_x < 0 \quad \text{on } \Pi_2(x,y) \tag{20}$$

$$t_y(x,y) = t_x(x,y) = 0 \quad \text{on } S_u \tag{21}$$

and essential

$$u_x(x,y) = u_y(x,y) = 0 \quad \text{on } S_d, S_r, S_l, S_u \tag{22}$$

$$u_x(x,y) < d_x(x,y) \quad \text{on } A(x,y) \tag{23}$$

$$u_y(x,y) < d_y(x,y) \quad \text{on } A(x,y) \tag{24}$$

where S_d, S_r and S_l are the surfaces of the rigid walls of the container, S_u the superior plane of the packed bed [Fig. 3(a)], A is the deformable external surface of the generic cylinder [Fig. 3(b)], n_x and n_y are the components (or direction cosines) of the unit normal vector at the contact area, Π_1 and Π_2 are the contact areas between the contiguous cylinders [Fig. 3(b)], t_y is the specific boundary stress caused by the weight of the laid-upon rows of cylinders, t_x is the specific boundary stress between the contiguous cylinders in the same row caused by the rigidity of the container walls, and dx and dy are the distances of a point of a cylinder from the nearest separation plane of two vertical and horizontal rows of cylinders, respectively [Fig. 3(b)].

The boundary conditions expressed by (23) and (24) contain the geometrical information necessary to impose non-penetration between the deformable cylinders.

We can now observe that the porous medium is characterized by a periodic and uniform structure defined by a unit cell. It is then possible to study the unit cell in order to evaluate the global (homogenized) behaviour of the packed bed. The problem is to identify the opportune boundary conditions to impose on the unit cell. In fact, considering the natural boundary conditions, we note that the weight force acting on any of the cylinders is different, and, consequently, the contact surfaces have different dimensions in relation to the height of the cylinder in the packed bed. To obtain the weight force to impose on the unit cell, we consider as boundary stresses on the contact areas those produced by the average weight force distributed along the height of the packed bed and acting in a direction normal to the area Π_1.

In the linear elastic hypothesis the average weight force can be easily evaluated as the arithmetic average of the weight forces applied on the first and the last cylinder of the packed bed. In this case, G is a function only of the radius of the cylinder, r, the density of the solid, ρ, and the number of rows of cylinders, N.

The natural boundary conditions on the single cylinder of the unit cell [Fig. 4(a)] are (19) and (20) whereas the essential boundary conditions are modified as:

$$u_x(x,y) = 0 \quad \text{on } x = \pm r \quad \text{and} \quad y = 0 \tag{25}$$

$$u_y(x,y) = 0 \quad \text{on } x = 0 \quad \text{and} \quad y = \pm r \tag{26}$$

$$u_x(x,y) \leqslant |r-x| \quad \text{on } r = (x^2+y^2)^{0.5} \quad \text{with } 0 \leqslant x \leqslant r \quad \text{and} \quad 0 \leqslant y \leqslant r \tag{27}$$

$$u_y(x,y) \leqslant |r-y| \quad \text{on } r = (x^2+y^2)^{0.5} \quad \text{with } 0 \leqslant x \leqslant r \quad \text{and} \quad 0 \leqslant y \leqslant r. \tag{28}$$

The boundary conditions are formulated assuming that the arch effect induced on each cylinder from the rigid constraints of the container walls is neglected.

The system of equations (14)–(18) with boundary conditions (19) and (20) and (25)–(28) was solved using the Galerkin finite-element method [15]. The discretization of the domain was developed using a bilinear quadrilateral and triangle linear planer elements.

Solution stability was obtained with a mesh of 10 000 elements in a quarter of the cylinder, while the contact area was discretized with about 30 elements.

Non-linear boundary conditions include contact problems, as well as non-linear support conditions. The procedure used for the solution of non-linear equations is the modified Newton–Raphson method. The convergence criterion is based on the magnitude of the maximum residual load compared to the maximum reaction force.

In the light of the numerical results obtained, the values of the width c_1 of the contact strip [Fig. 4(a)] can be obtained to a good approximation using the theory proposed by Hertz [14], valid for the following simplifying hypotheses: (i) elastic and isotropic solids; (ii) forces acting in an orthogonal direction to the contact surfaces (this hypothesis is verified since the only force acting is the weight force); (iii) strains being much smaller than the cylinder radius; and (iv) the cylinder being fixed by the presence of the cylinders above and below, but free to deform laterally.

In this hypothesis, it is possible to obtain the expression of the width c_1 of the contact strip as:

$$c_1 = 4 \cdot \sqrt{\left(\frac{G \cdot r \cdot (1-\nu^2)}{\pi \cdot E}\right)}. \tag{29}$$

In a packed bed, hypothesis (iv) is not verified for the presence of lateral cylinders but if the weight forces act on each cylinder are not very high, the corresponding width c_2 of the lateral contact strip [Fig. 4(a)] are neglected (Fig. 6) and, therefore, the values of c_1 obtained using the numerical method coincide with the analogous values calculated using the simplified relationship (29). In particular, the maximum percentage difference is equal to 0.4% in correspondence to an H-value equal to 60 cm.

The average weight force G and the packing height H are equal to $\frac{1}{2}(\rho\pi r^2 L_c N)$ and $2Nr$ respectively, where L_c is the length of cylinders; substituting these expressions in (29), it can be seen that, for the same material, the $c_1 : r$ ratio proves to be a function only of H. Consequently, in hypothesis (i), the $c_2 : c_1$ ratio is a function only of the packing height for the same material.

The results of the numerical simulations are shown in Figs. 5 and 6. In particular ratios $c_1 : r$ and $c_2 : r$ are given as a function of the height of the packed bed for a number of different solid materials.

2.2. *The thermal problem*

The resolution of the thermal problem is based on the simple consideration that the effective conductivity can also be computed directly by using the temperature field. In particular $\mathbf{K}_e$ can be obtained from:

$$\langle q \rangle = -\mathbf{K}_e \nabla \langle T \rangle \tag{30}$$

where in the particular case of the isotropic porous medium the tensor $\mathbf{K}_e$ becomes a scalar k_e [16].

The temperature field can be obtained resolving the system of differential equations (1) with the boundary conditions represented by (2) and by the other boundary conditions on the regular packed bed of circular cylinders [Fig. 3(a)], which are:

$$\frac{\partial T(x,y)}{\partial x} = 0 \quad \text{on } S_r \quad \text{and} \quad S_l \tag{31}$$

$$T(x,y) = T_u \quad \text{on } S_u \tag{32}$$

$$T(x,y) = T_d \quad \text{on } S_d. \tag{33}$$

For symmetric conditions the temperature field in the porous medium can be obtained from the temperature field calculated only in the unit cell of Fig. 4(a) with the boundary conditions:

$$\frac{\partial T(x,y)}{\partial x} = 0 \quad \text{for } x = \pm\frac{L}{2} \quad \text{and} \quad -\frac{L}{2} \leqslant y \leqslant \frac{L}{2} \tag{34}$$

$$T(x,y) = T_1 \quad \text{for } y = \frac{L}{2} \quad \text{and} \quad -\frac{L}{2} \leqslant x \leqslant \frac{L}{2} \tag{35}$$

$$T(x,y) = T_2 \quad \text{for } y = -\frac{L}{2} \quad \text{and} \quad -\frac{L}{2} \leqslant x \leqslant \frac{L}{2} \tag{36}$$

where:

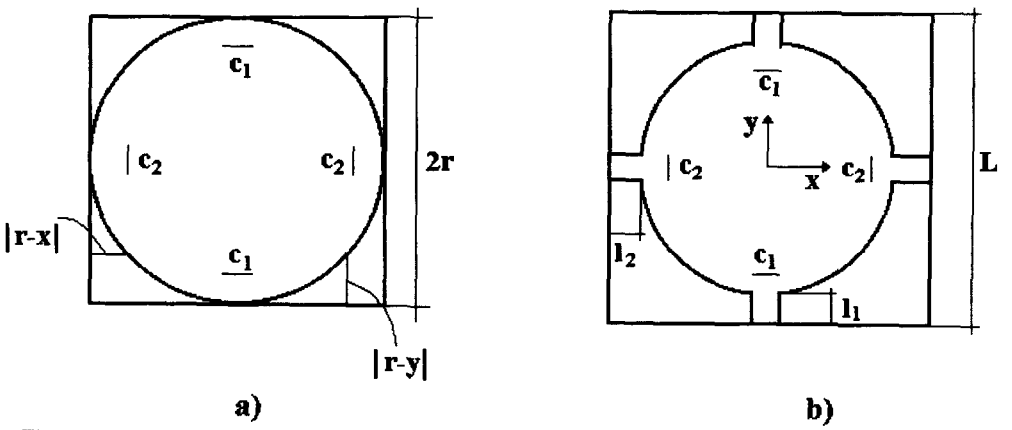

Fig. 4. (a) Unit cell for interconnected circular cylinders, (b) modified unit cell for interconnected circular cylinders.

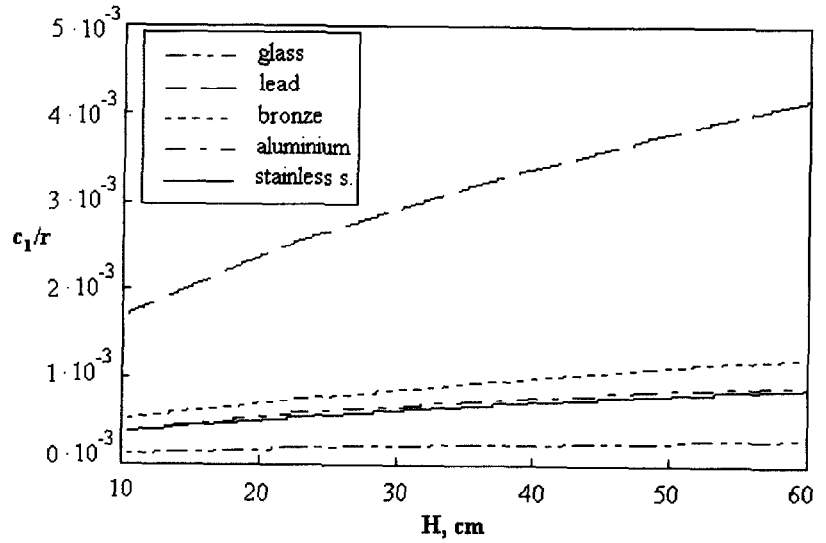

Fig. 5. c_1 width in relation to the height of the regular packed bed for different materials.

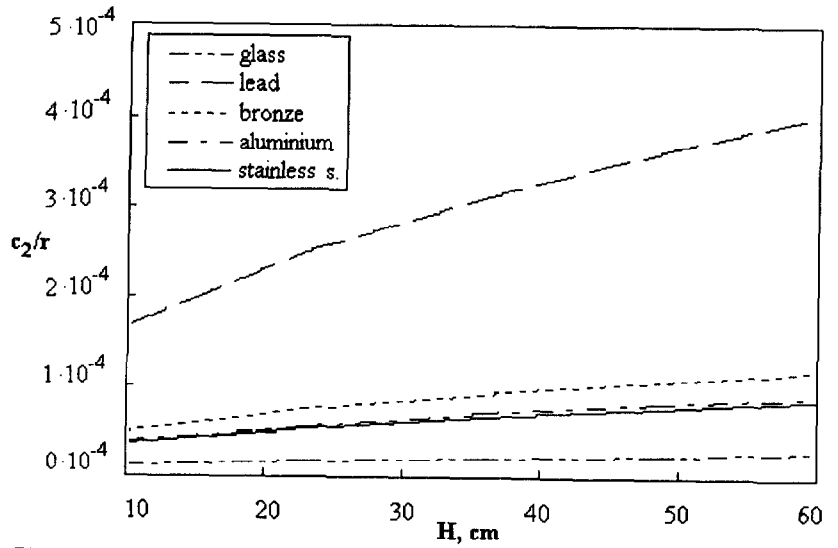

Fig. 6. c_2 width in relation to the height of the regular packed bed for different materials.

$$\Delta T = T_1 - T_2 = \frac{T_u - T_d}{N}. \tag{37}$$

Equation (37) can be obtained from simple considerations on the symmetry of the field of temperature of the regular packed bed with the boundary conditions (31), (32) and (33) and on the periodicity of the unitary cell. In fact, the field of temperature in the unitary cell is periodic along the Y-axis [apart from the ΔT that can be obtained from (37)] and periodic along the X-axis for the whole regular packed bed.

Assuming that k_e does not vary with temperature (i.e. k_s, k_f and ϕ are independent from temperature) the value of the effective conductivity can be calculated as:

$$k_e = -\frac{\langle q \rangle}{\nabla \langle T \rangle} = -\frac{L}{V}\frac{\int_V q \, dV}{\Delta T}. \tag{38}$$

The numerical solution of the integral in (38) can be easily obtained from the temperature field when this is determined using the Galerkin Finite Element Method. In fact the components of the heat flux can be calculated for each element using the Gauss–Legendre quadrature [15].

The mesh used to solve the thermal problem in the solid cylinder is obtained from the mesh used in the solid mechanics problem modifying the positions of the nodes to take account of the displacement field.

The values of effective thermal conductivity obtained using the proposed method proved, however to be always significantly larger than the experimental values of k_e proposed in literature.

The over-estimation of these results depends on having neglected the imperfect nature of the contact area between the cylinders. The roughness of the surfaces determine the presence of voids in the real contact area. These discontinuities cause an additional thermal resistance, called the thermal contact resistance, which manifests itself as a temperature drop at the interface. The magnitude of this thermal resistance depends on the surface roughness, the type of material, the interface pressure, the interface temperature and the type of fluid filling the voids.

In particular the additional thermal resistance is strongly influenced by the surface behavior in contact, which varies according to the asperity deformations which can be elastic, plastic or elasto-plastic.

The deformation properties of a rough surface is described by the plasticity index Ψ. In this study we use the definition of Ψ proposed by Mikic [17]:

$$\Psi = \frac{2 \cdot \delta \cdot (1 - \nu^2)}{E \cdot \tan \vartheta_m} \tag{39}$$

where ϑ_m is the average angle of inclination of the faces of the asperities on the surface of the solid and δ is the hardness of the material. If the value of Ψ is appreciably less than unity, the deformation of the asperities will be entirely plastic; if the value is greater than unity the deformation will be predominantly elastic. In this study we consider that the deformations of the asperities are entirely elastic.

Consequently the proposed method is approximately valid for ϑ_m being lower than material type characteristic values; for example, for stainless steel and aluminium with a probability of 90% the deformation of the asperities is elastic for ϑ_m lower than *ca* 80°, whereas with a probability of 95–99.7% the deformation is elastic for ϑ_m being lower than respectively *ca* 45° and 20° [17].

For elastic deformations of the asperities in the contact area, Mikic in [17] proposed the following theoretical relationship to calculate the thermal contact conductance:

$$h = 1.9 \frac{k_s}{\xi} \left(\frac{2P(1 - \nu^2)}{E} \right)^{0.94} \tag{40}$$

where ξ is the roughness of the material and P is the pressure on the nominal contact area. Equation (40) is valid for a thermal conductivity of the fluid much lower than k_s in order to be able to neglect the thermal flow passing through the voids present in the contact area.

Equation (40) cannot be used in a boundary condition to determine the temperature field in the unit cell since the temperature profiles on the two sides of the contact interface are both unknowns. Moreover, since the thermal contact resistance is a function of the pressure on the nominal contact area, it varies in relation to the position of the cylinder under investigation. Analogously to the solid mechanics problem, the thermal problem should be solved for the entire geometrical domain of the porous medium. Hence, the unit cell model can be again applied only by introducing some approximations. In particular, in an analogous manner to the one proposed by Nozad *et al.* [7], the unit cell is modified as shown in Fig. 4(b). The contact effect is again simulated using two different slabs placed in the centre of the side of the unit cell. The dimensions, c_1 and c_2, of the slabs are equal to the dimensions of the respective nominal contact areas and are, therefore, obtained from the resolution of the system of equations (14)–(18) with boundary conditions (19) and (20) and (25)–(28), whereas the lengths l_1 and l_2 of the slabs are determined using an iterative procedure. The first attempt values of l_1 and l_2 are calculated making the thermal resistance of the area added to the unitary cell equal to the mean contact thermal resistance R_1 calculated assuming monodimensional heat flux:

$$h_1 c_1 \cdot 1 = \frac{k_s c_1}{l_1} \cdot 1 + \frac{k_f (L - c_1)}{l_1} \cdot 1. \tag{41}$$

h_1 is determined introducing the pressure P_1, calculated as the ratio of the average weight force G and the nominal contact area Π_1 into (40). Thus:

$$l_1 = \frac{(k_s c_1 + k_f(L - c_1))}{h_1 c_1} = \frac{k_s}{h_1} + \frac{k_f(L - c_1)}{h_1 c_1} \quad (42)$$

and:

$$l_1 = l_2. \quad (43)$$

The unitary cell is constructed in relation to the first attempt values l_1 and l_2, and therefore, the temperature field is determined resolving the system of equations (1) with the boundary conditions (2) and (34)–(36); finally the effective thermal conductivity is calculated using equation (38). Lengths l_1 and l_2 are iteratively modified until the thermal resistances R_1 or R_2 of the areas added to the unitary cell calculated by means of:

$$R_1^{-1} = \int_{x=-L/2}^{x=L/2} \frac{q(x,y)}{T\left(x, y = \frac{L}{2}\right) - T\left(x, y = \frac{L}{2} - l_1\right)} \mathrm{d}x \quad (44)$$

$$R_2^{-1} = \int_{y=-L/2}^{y=L/2} \frac{q(x,y)}{T\left(x = \frac{L}{2}, y\right) - T\left(x = \frac{L}{2} - l_2, y\right)} \mathrm{d}y \quad (45)$$

are equal to the contact resistances to an approximation of 0.2% in terms of k_e.

Note that equations (42)–(45) are formulated for the case of the temperature gradient imposed as the boundary condition being parallel to the Y-axis, and, therefore, having the same direction as the weight force G. If this gradient is parallel to the X-axis, the values of k_e prove to be different since the thermal contact resistances are varied; in particular, for equal imposed temperature gradients, the contact area being lower, the values of k_e will be lower compared to the previous ones. Analogous equations to (42)–(45) can however be easily determined.

Note, furthermore, that in the case of ∇T being parallel to the Y-axis, the values of k_e calculated assuming the lengths of all the slabs to be equal to l_1, coincide with the ones calculated using the above described procedure which differences the slabs dimensions. This can be explained since the contact area Π_2 does not have a large influence from the thermal point of view in calculating k_e in the case of ∇T being parallel to the Y-axis and the material behaving in an elastic manner. In this case, it follows that if the values of c_1 can be determined using (29), the values of k_e can be determined resolving only the field of temperature in the unitary cell.

Vice versa, in the case of ∇T being parallel to the X-axis, it is indispensable to resolve the system of differential equations (14)–(18) with the boundary conditions (19) and (20) and (25)–(28) to determine the dimensions, c_2, of the contact strip and of the pressure P_2.

3. RESULTS

The method proposed to calculate the effective thermal conductivity was applied to the case of regular packed bed of stainless steel and aluminium cylinders. The application is obviously subordinated to knowing the mean value of roughness to be introduced into (40). Regarding this, it must be specified that this value is in relation to the superficial processing carried out on the material. Excluding rough superficial machining or superficial processing that leaves very low roughness (lapping, buffing, etc.), only the machining considered to be probable in the absence of precise indications (grinding) was taken into account. This machining is, however, characterized by a wide roughness range (2–60 μm). Thus, the machining is indicated using the terms fine, medium and coarse in relation to the superficial finish obtained (Table 1).

Regarding the applications under examination, it should be underlined that coarse aluminium gives much higher roughness values compared to stainless steel. Furthermore, the technologies for producing cylinders and full spheres are much more consolidated for stainless steel than for aluminium (for example one can consider the consolidated technology of stainless steel for the ball bearings and heat exchangers).

Consequently, the roughness calculation limit values for stainless steel were assumed for the fine machining range, whereas for aluminium the limit values were assumed for the medium and coarse machining ranges.

The values of k_e obtained applying the above-indicated calculation method, are given in Figs. 7 and 8 for a regular packed bed of stainless steel circular cylinders in relation both to the height H of the bed, and to variations in the roughness, for ∇T being parallel to the Y and X-axes, respectively. Figure 9 shows on the other hand, the values of k_e in relation to H and as the roughness ξ varies for a regular packed of aluminium circular cylinders only for ∇T being parallel to the Y-axis. The other case was not examined because of the lack of any experimental value even of a qualitative nature. Finally, it should be noted that the maximum packed height examined in Fig. 9 is of 0.60 m since, assuming a yield stress of 20 MPa, greater heights would give rise to macroscopical plasticization of the lower aluminium cylinders and, therefore, the proposed method could not be applied. As far as the calculation method is concerned, it must be underlined that:

(1) the increases in the area of the unitary cells,

Table 1. Ranges of roughness in relation to the type of machining

Type of machining	ξ [μm]
Fine	2–8
Medium	8–16
Coarse	16–60

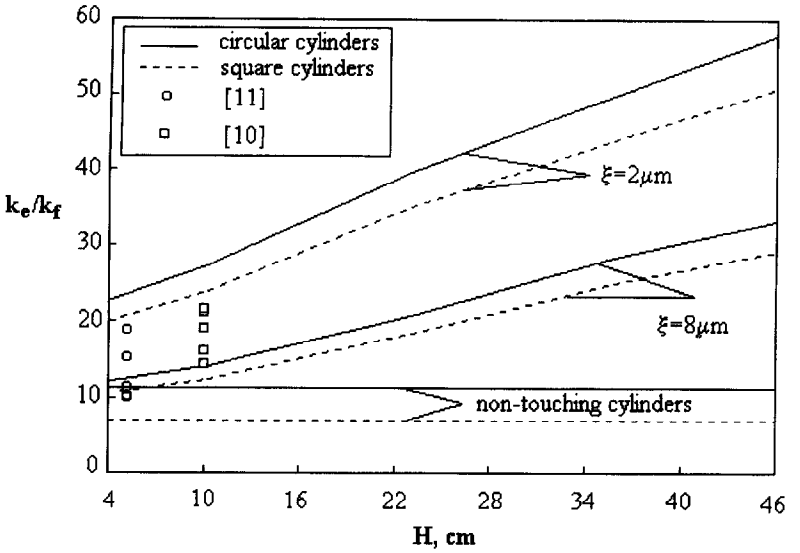

Fig. 7. The effective thermal conductivity for a bed of circular (continuous line) and square (dashed line) stainless steel cylinders with thermal gradient along the Y-axis in relation to the height of the regular packed bed, H, and the roughness of the solid particles, ξ.

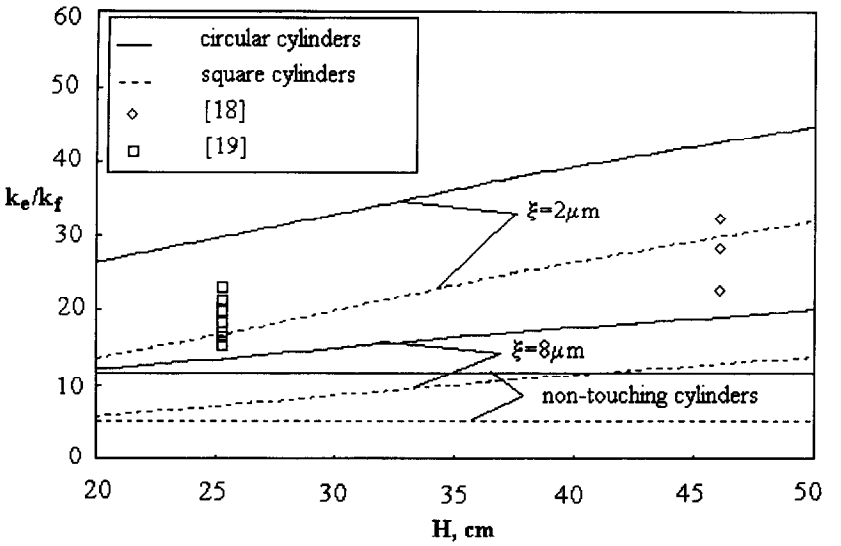

Fig. 8. The effective thermal conductivity for a bed of circular (continuous line) and square (dashed line) stainless steel cylinders with thermal gradient along X-axis in relation to the height of the regular packed bed, H, and the roughness of the solid particles, ξ.

included to take account of the thermal contact resistances, slightly modify the porosity values of the packed bed ($\phi = 0.22$); in particular, in the case of the porous matrix made up of stainless steel cylinders the maximum porosity value proves to be equal to 0.24 whereas in the case of aluminium this maximum value is equal to 0.27;

(2) for a packed bed of stainless steel cylinders, the iterative procedure to calculate l_1 and l_2 can be avoided to a good approximation. In fact, the values of k_e obtained assuming the lengths l_1 and l_2 to be equal to the first attempt values, when calculated differ, at most, by 2% compared to the values of k_e obtained using the iterative procedure. Vice versa, for the aluminium cylinders, this approximation determines a maximum percentage difference of 6%.

From Figs. 7–9, it can be seen that, for H and ξ being equal and the conductivity of the stainless steel being less than that of the aluminium, the values of k_e prove to be less for the porous particles made up from cylinders of stainless steel. Furthermore, in the case of these cylinders, for equal roughness, the values of k_e prove to be greater for the temperature gradient being parallel to the Y-axis than is the case for ∇T being parallel to the X-axis. This behaviour depends on the fact that as H increases, the dimensions of the contact area Π_1 (Figs. 5 and 6) increase more than

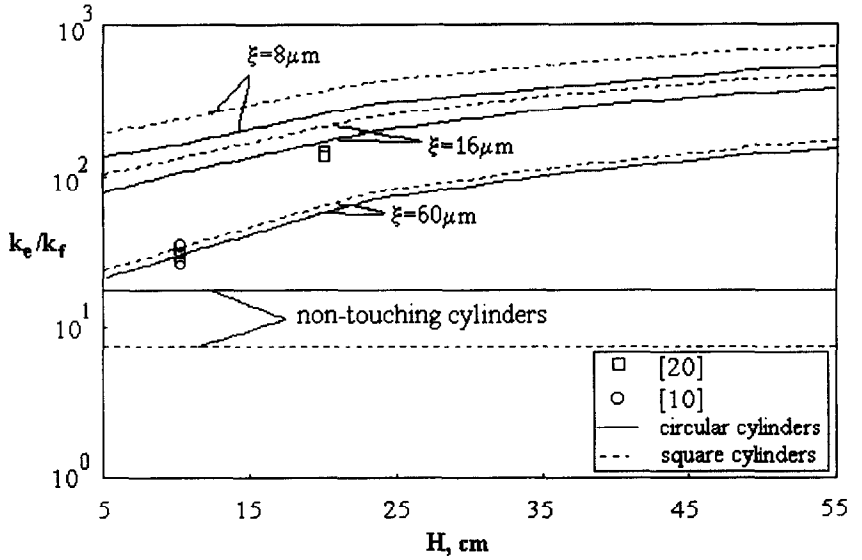

Fig. 9. The effective thermal conductivity for a bed of circular (continuous line) and square (dashed line) aluminium cylinders with thermal gradient along the Y-axis in relation to the height of the regular packed bed, H, and the roughness of the solid particles, ξ.

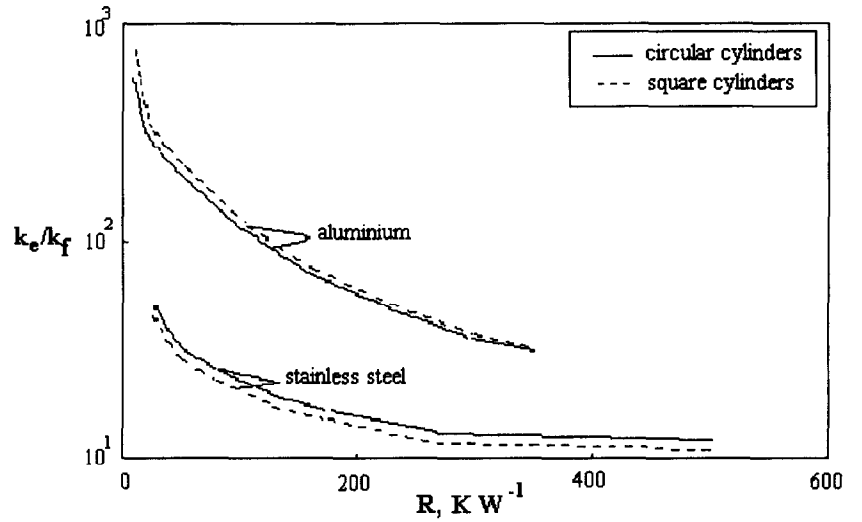

Fig. 10. The effective thermal conductivity in relation to the thermal contact resistance, R, for different materials.

those of the contact area Π_2. Hence, when the temperature gradient is parallel to the Y-axis, the value of k_e is greater than when the temperature gradient parallel to the X-axis, for all other parameters being equal. This proves that k_e not only depends on the dimensions of the contact area, but also on the orientation of these areas compared to the temperature gradient.

Figure 10 shows the values of the ratio $k_e : k_f$ in relation to the contact thermal resistance for steel and aluminium cylinders. This diagram shows how as the roughness decreases (and therefore the thermal resistance) the value of k_e increases. The maximum value of k_e can be obviously obtained when the contact area is equal to the corresponding nominal contact area.

Sahraoui and Kaviany [9] studied the effect of particle shape on k_e for non-touching circular and square cylinders. They underline that the particle shape becomes significant only as the porosity decreases ($\phi < 0.5$). We investigated this influence for touching cylinders in a similar manner, comparing the values of k_e for circular and square cylinders for equal porosity and contact resistances. The effective conductivity values determined using the unit cell shown in Fig. 2(c) are indicated in Figs. 7–9 by the dashed line.

From the comparison, it can be seen that the difference between the values of k_e in both cases examined is not negligible and that this difference remains approximately constant as H varies for equal material roughness. The difference found in the values of k_e depends on the contact thermal resistance. In fact, the

Table 2. Experimental data reported in literature

Porous medium	Ref.	Arrangement	ϕ	H [mm]	ΔT direction	k_s/k_f
Stainless steel spheres—air	[18]	Random	0.39–0.43	465	X	2385
Stainless steel spheres—air	[11]	Simple cubic array	0.52	52	Y	1650
Stainless steel spheres—air	[19]	Random	0.49	500	X	1646
Stainless steel circular cylinders—air	[19]	Random	0.40	250	Y	1646
Stainless steel spheres—air	[10]	Simple cubic array	0.52	100	Y	614
Aluminium spheres—air	[10]	Simple cubic array	0.52	100	Y	6325
Aluminium spheres—air	[20]	Random	0.40–0.41	200	Y	8077

difference in the values of k_e of the two cells in Fig. 2(c) and Fig. 4(b) increases as the roughness decreases and, therefore, the contact thermal resistance. Furthermore, comparing Figs. 7 and 8, indicates that this difference proves to be greater for temperature gradient parallel to the Y-axis, for all other parameters being equal.

Hence the influence of solid particles shape in a porous medium tends to diminish as the contact thermal resistance increases.

The absence of experimental data for a regular packed bed of cylinders does not permit verification of the proposed model. As is reported in [7] and in [9], comparison with the experimental data obtained with different porosities and geometries, can in any case be indicative of the suitability of the model. We must emphasize that this comparison is exclusively qualitative since it is carried out between numerical results determined practically with porosity values comprised between 0.22 and 0.27 and experimental results regarding values of ϕ comprised between 0.40 and 0.52. In any case some interesting considerations can be made.

The experimental conditions for the observations that have been examined and reported in the literature are summarized in Table 2 and the measurement values of $k_e : k_f$ are shown in Figs. 7–9.

From the examination of these figures, even if the roughness values of the materials used for the experiments are not known, it can be deduced that the variations of this parameter can be the cause of both the scatter in the data measured in apparently the same experimental conditions, and the large difference between the experimental data of k_e in the case of aluminium.

4. CONCLUSIONS

A method to calculate the effective thermal conductivity of a two-phase isotropic porous medium with touching particles is presented. This method, based on the volume averaging technique, determines the values of the effective thermal conductivity including the details of the solid mechanics and thermal problems.

The methodology is applied for periodic regular arrangements of circular and square cylinders. The effects of particle shape, roughness and solid conductivity are examined. Unfortunately the particular type of porous medium examined does not permit the influence of the porosity on the effective thermal conductivity to be evaluated. The indispensable evaluation of the influence of this parameter as well as the number and the position of the contact areas, will be the next objectives to be reached. In particular, the authors wish to apply their method to the case of a 3D porous medium made up of spheres with a different type of arrangement, in particular a simple cubic array and a body-centred cubic array.

REFERENCES

1. S. Whitaker, Simultaneous heat, mass and momentum transfer in porous media: a theory of drying, *Adv. Heat Transfer* **13,** 119–203 (1977).
2. R. G. Carbonell and S. Whitaker, Heat and mass transfer in porous media. In *Fundamental of Transport Phenomena in Porous Media* (Edited by J. Bear and M. Y. Corapcioglu), pp. 121–198. Martinus Nijhoff, Dordrecht (1984).
3. S. Whitaker, Improved constraints for the principle of local thermal equilibrium, *Ind. Engng Chem. Res.* **30,** 983–987 (1991).
4. S. Whitaker, Diffusion and dispersion in porous media, *A.I.Ch.E. J.* **13,** 420–427 (1967).
5. W. G. Gray, A derivation of the equation for multiphase transport, *Chem. Engng Sci.* **30,** 229–233 (1975).
6. Y. Bachmat and J. Bear, On the concept and size of a representative elementary volume. In *Advances in Transport Phenomena in Porous Media* (Edited by J. Bear and M. Y. Corapcioglu), pp. 121–198, Martinus Nijhoff, Dordrecht (1987).
7. I. Nozad, R. G. Carbonell and S. Whitaker, Heat conduction in multiphase system—I, *Chem. Engng Sci.* **40,** 843–855 (1985).
8. D. Ryan, R. Carbonell and S. Whitaker, Effective diffusivities for catalyst pellets under reactive conditions, *Chem. Engng Sci.* **35,** 10–16 (1980).
9. M. Sahraoui and M. Kaviany, Slip and no-slip temperature boundary conditions at interface of porous, plain media: conduction, *Int. J. Heat Mass Transfer* **37,** 1029–1044 (1994).
10. D. R. Shonnard and S. Whitaker, The effective thermal conductivity for a point contact porous medium, *Int. J. Heat Mass Transfer* **32,** 503–512 (1989).
11. E. F. Jaguaribe and D. E. Beasley, Modelling of the effective thermal conductivity and diffusivity of a packed bed with stagnant fluid, *Int. J. Heat Mass Transfer* **27,** 399–407 (1984).
12. G. K. Batchelor and R. W. O'Brien, Thermal or electrical conduction through a granular material, *Proc. R. Soc. Lond. A* **355,** 313–333 (1977).

13. K. L. Johnson, *Contact Mechanics*, Chaps. 4 and 9. Cambridge University Press, Cambridge, U.K. (1992).
14. A. E. Saez, J. C. Perfetti and I. Rusinek, Prediction of effective diffusivities in porous media using spatially periodic models, *Transp. Porous Media* **6,** 143–157 (1991).
15. J. N. Reddy, *An Introduction to the Finite Element Method* (2nd Edn), Chaps. 7, 9 and 10. McGraw-Hill, New York (1993).
16. M. Kaviany, *Principles of Heat Transfer in Porous Media*, Chap. 3. Springer, New York (1991).
17. B. B. Mikic, Thermal contact conductance: theoretical considerations, *Int. J. Heat Mass Transfer* **17,** 205–214 (1974).
18. M. M. Melanson and A. G. Dixon, Solid conduction in low d_t/d_p beds of spheres, pellets and rings, *Int. J. Heat Mass Transfer* **28,** 383–394 (1985).
19. A. L. Waddams, The flow of the heat through granular material, *J. Soc. Chem. Ind.* **63,** 336–340 (1994).
20. I. Nozad, R. G. Carbonell and S. Whitaker, Heat conduction in multiphase system—II, *Chem. Engng Sci.* **40,** 857–863 (1985).